Morphology and Local Dynamics in a Series of Aromatic Terpolyesters

U. Wiesner,† F. Lauprêtre,* and L. Monnerie

Laboratoire de Physicochimie Structurale et Macromolèculaire Associé au C.N.R.S., E.S.P.C.I., 10 rue Vauquelin, 75231 Paris Cédex 05, France

Received September 24, 1993; Revised Manuscript Received March 27, 1994®

ABSTRACT: The molecular morphology and the local dynamics of a series of aromatic terpolyesters based on *p*-hydroxybenzoic acid, hydroquinone, and isophthalic acid were investigated using X-ray diffraction and high-resolution solid-state ^{13}C NMR. Correlations between the existence of well-defined crystalline forms and the local mobility of the individual polymer units were established. In certain cases, polymers containing less than 30% *p*-hydroxybenzoic acid exhibit a crystalline reorganization upon annealing, giving rise to a change in the dominant crystalline form. The ^{13}C chemical shift tensor parameters were determined from the spinning sideband intensities for the polymers containing 27 and 80% *p*-hydroxybenzoic acid. Depending on the temperature, two types of molecular motions were observed for the *para*-substituted phenyl rings. At low temperatures, there first occur ring oscillations around the *para* axis; then, at higher temperatures, small-amplitude main-chain reorientations are involved in the glass transition phenomena. In addition to these findings, a postcondensation with an attendant increase in molecular weight was detected under annealing for these polymers.

Introduction

In recent years stiff-chain thermotropic polymers have become of increasing interest for their ability to form high-performance engineering resins and high-strength, high-modulus fibers and moldings. Many aspects of the synthesis and behavior of these materials have already been examined and a number of reviews exist.[1,2]

To exhibit a mesomorphic behavior and at the same time to be processable within the industrially convenient melt temperature zone of 523–583 K, several molecular designs have been developed for thermotropic liquid crystal polymers (LCP's). The general approach is to disrupt the regularity of the often intractable polymers, thereby lowering the crystal–nematic transition temperature and improving the solubility. For example, in *para*-linked polyesters, disruption can be achieved by inducing an arrangement referred to as "frustrated chain packing". The interchain distance is increased by using bulky substituents or the interchain atomic registry is broken by copolymerizing monomers with different molecular dimensions. Alternatively, the regularity may be disrupted by the incorporation of nonlinear links like *meta*- or *ortho*-substituted phenyl rings or other "kinked" monomer units into the polymer backbone.

The above-mentioned requirements have moved industrial research on thermotropic LCP's mainly toward fully aromatic copolyesters or amides. A number of such polymers have been intensively studied and are now commercially available.[3] In these systems the rodlike shape is a consequence of the hindered rotation around the ester or amide bond.[4-6] Alternatively, mainly in academic research, new and interesting ways have been found to introduce stiffness into the polymer chain using for example steric interactions of neighboring monomers[7,8] or suitable geometries in cycloaliphatic structures.[9]

Typical representatives of LCP's based on "kinks" and "frustrated chain packing" are the terpolyester built from *p*-hydroxybenzoic acid (HBA), hydroquinone (HQ), and angular isophthalic acid (IA) and the copolyester from *p*-hydroxybenzoic acid and hydroxynaphthoic acid (HNA), respectively. A comparison of the behavior of these two polymers indicates that the polymer architecture has major implications for the bulk polymer properties. Whereas the former copolyester forms crystals with good 3D order and possesses values for the heat and the entropy of fusion (ΔH_f and ΔS_f) close to those observed in conventional isotropic polymers such as poly(ethylene terephthalate) (PET), the latter forms crystals of poor 3D order and the values of ΔH_f and ΔS_f are significantly lower.[10,11] Since chain packing in the crystalline regions influences polymer density, these observations have important implications for the macroscopic properties of the LCP's like warpage and shrinkage in molding.[12] In addition, local dynamical properties are markedly different. The LCP based on kinks does not exhibit the β loss process associated with the naphthyl moieties in the copolymer of hydroxybenzoic acid and hydroxynaphthoic acid, resulting in a better modulus retention at higher temperatures.[13] It thus appears that the knowledge of molecular parameters such as order and dynamics in the bulk is of great importance in relating molecular structure to macroscopic behavior.

The present work deals with the terpolyester prepared from *p*-hydroxybenzoic acid, hydroquinone, and angular isophthalic acid in varying proportions. The stoichiometric formula may be depicted as follows:

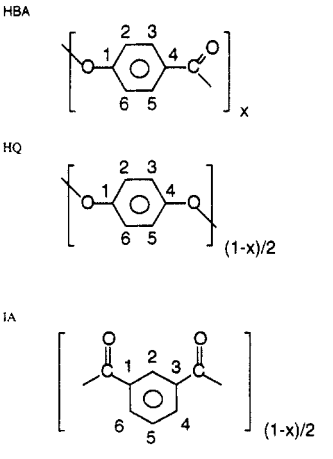

In this polymer series the molar fractions of isophthalic

† Permanent address: Max-Planck-Institut für Polymerforschung, Postfach 3148, 55021 Mainz, Germany.

® Abstract published in *Advance ACS Abstracts*, May 15, 1994.

0024-9297/94/2227-3632$04.50/0

acid and hydroquinone are equal and the remainder is made up of *p*-hydroxybenzoic acid. Although in the middle composition range this LCP has superior modulus retention with increasing temperature than the naphthalene-containing LCP, compared to similar isotropic aromatic polyesters, its modulus retention at temperatures between 273 and 393 K is rather poor.[13] The glass transition temperature, T_g, of the system lies at the upper limit of this range. In an earlier study, we used high-resolution solid-state ^{13}C NMR to investigate the nature of the local motions that are responsible for the observed secondary relaxations in the particular example of the almost entirely amorphous terpolyester with $x = 0.33$.[14]

The purpose of the present work is to extend our study to a broader composition range of the terpolyester including highly crystalline materials. Earlier works of Erdemir *et al.*[15] and Blundell *et al.*[11] have shown the complex phase behavior exhibited by the terpolymer as a function of the HBA content. Compositions containing low amounts of HBA ($x < 0.2$) are conventional semicrystalline polymers showing no mesomorphic characteristics. Polymers in the range $0.2 < x < 0.27$ are borderline cases between isotropic and liquid crystalline behavior. Compositions in the range $0.3 < x < 0.5$ exhibit a large nematogenic temperature range. Terpolyesters with higher HBA contents ($x > 0.6$) tend to be intractable and decompose at temperatures below their crystal–nematic transition.

Results reported in this paper are based on high-resolution solid-state ^{13}C NMR experiments performed at different temperatures above and below the glass transition temperature. Using the method of Herzfeld and Berger,[16] the motional modulation of the chemical shift anisotropy of the different carbons is followed. In this way the dynamic behavior of the different aromatic units can be determined as a function of the composition. Since in the lower and upper concentration ranges of *p*-hydroxybenzoic acid the polymer is highly crystalline, the results will be correlated with those of X-ray diffraction experiments. In particular, the nature of the monomeric units located in the crystalline and amorphous regions, respectively, should be clearly evidenced using solid-state NMR. Indeed, almost no motions are expected to occur in the crystalline phases below the melting temperature, whereas in the amorphous regions we should observe some mobility related to secondary transitions below T_g and processes associated with the glass transition above T_g. Special attention will be focused on the effects of prolonged annealing on the crystallinity since it has been observed[17,18] that, at temperatures between the glass and the crystal–nematic transition, crystalline reorganization takes place. Furthermore, we investigate whether a postcondensation of the polyester with an attendant increase in molecular weight can take place during the annealing experiments or the long accumulation times necessary to collect high-resolution NMR spectra at high temperatures. Therefore, the first part of this paper will be devoted to thermogravimetric, calorimetric, and viscosity measurements on one particular sample as a function of the annealing parameters.

Experimental Section

Materials. The five terpolyesters with $x = 0.17$, 0.21, 0.27, 0.33, and 0.80 (denoted HBA17 up to HBA80 in the text) were synthesized by F. Beaume, W. A. MacDonald, and N. Clough at the I.C.I. Wilton Research Centre in Great Britain. They were prepared using a novel nonaqueous dispersion process described in ref 11. The polymers are obtained from this technique in an unsheared quiescent state.

Polymer Characterization. Thermal stabilities were assessed by thermogravimetric analysis (DuPont 9900–TGA 951) carried out under a nitrogen atmosphere.

The transition temperatures were measured using a differential scanning calorimeter (DSC) (DuPont 1090) operating at 20 K/min. The glass transition temperature, T_g, was estimated from the intersection between the initial base line and the sloping portion of the base line due to the glass transition phenomena.

Specific solution viscosities of polymers were measured in a 30/70 (v/v) mixture of trifluoroacetic acid and dichloromethane at 298 K using a capillary Ostwald type viscosimeter. The concentration of the solutions was 3 g/L.

Dynamic mechanical properties were determined using a DuPont DMA983 dynamic mechanical analyzer. Experiments were performed at 0.1 and 1 Hz, the applied strain being in flexural mode.

Heat Treatments. The samples used for the investigation of the postcondensation were heated for about a day under vacuum at the following temperatures: 483, 503, 528, 553, 568, and 588 K. Samples used in the X-ray diffraction experiments were annealed at 510 K for different periods of time as described in the discussion. Prior to the NMR experiments, the investigated samples were heated at 510 K for about 20 h under vacuum. To check the influence of the absence or presence of vacuum in the heat treatment, we performed NMR measurements not only on the latter samples but also on those used for the X-ray experiments which were not annealed under vacuum. As expected, no difference in the local dynamics of the different samples was detected.

X-ray Diffraction Experiments. Samples for diffractometer scans were prepared by fixation of ground polymer powder on glass plates using a thin layer of vaseline. Scans were obtained in reflection using the Bragg–Brentano setup (λ(Cu Kα)). All measurements were performed at room temperature. To match the different diffractograms with the background diffraction from the noncrystalline regions of the amorphous polymer with $x = 0.33$, each recorded diffractogram was multiplied by an appropriate factor.

CP/MAS ^{13}C NMR Experiments. The high-resolution solid-state ^{13}C NMR experiments were carried out on nonoriented powder samples of the different polymers. The experiments were conducted at 75.47 MHz with a Bruker CXP 300 spectrometer, with quadrature detection and a single rf coil which was double tuned for both ^{13}C and ^{1}H. Proton dipolar decoupling (DD) and magic angle sample spinning (MAS) were used. The samples were contained in Al_2O_3 rotors. The spinning speed was around 4100 Hz. The pulse sequence consisted of a cross-polarization (CP) proton dipolar decoupling sequence. The matched spin-lock cross-polarization transfers were carried out with ^{13}C and ^{1}H magnetic field strengths of 64 kHz. The contact duration was 1 ms. The variable-temperature experiments at 75.47 MHz were made using a Doty probe. Spin-temperature inversion techniques allowed the minimization of base line noise and roll.[19] Flipback was used to shorten the delay time between two successive pulse sequences,[20] which was taken as 2.5 s. At higher temperatures, up to 30 000–35 000 scans were accumulated.

Results and Discussion

Postcondensation. For the postcondensation investigation the polymer with $x = 0.27$ (HBA27) was used since it is completely soluble in a 30/70 (v/v) mixture of trifluoroacetic acid and dichloromethane and therefore accessible to viscosity measurements. Thermal stabilities were observed at three different temperatures, 533, 553, and 573 K, all between T_g at 409 K and the onset of the melting peak at 593 K of the untreated polymer. A representative thermogravimetric curve recorded at 573 K for about 20 h is shown in Figure 1. As expected for a postcondensation, the weight of the sample decreases continuously as a function of time, the total weight loss increasing with the annealing temperature. The average number of monomer units per chain of the initial untreated polymer can be roughly estimated from the total loss at very long times, obtained from a fit of the observed decay

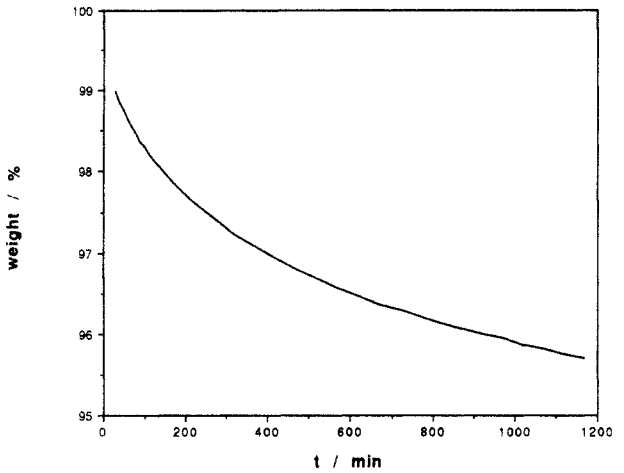

Figure 1. TGA curve of the HBA27 polymer at 573 K as a function of time. The onset is not exactly at 100% since during the first 20 min of the measurement the apparatus is equilibrated but the associated loss curve is not recorded.

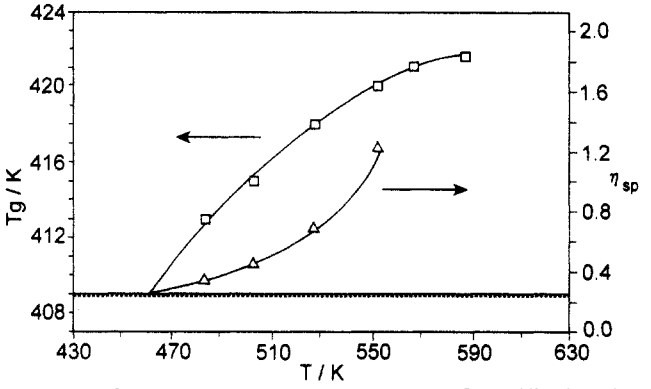

Figure 2. Glass transition temperature (□) and specific viscosity (△) of the HBA27 polymer as a function of the annealing temperature. T_g and η_{sp} of the untreated polymer are indicated as straight and dashed horizontal lines, respectively. The lines connecting the data points are a guide for the eye.

curve in Figure 1. A necessary condition for the calculation is that no degradation takes place, or, in other words, that the decay is entirely due to a loss of acetic acid from the acetoxyaryl groups at the chain ends. This is indeed the case as shown by dilute-solution light scattering measurements on this polymer before and after heating at temperatures up to 20 deg below the melting point, T_f.[17] Using further the assumption that the postcondensation takes place all the way up to the theoretical end of one final macromolecule, an average number of 10 monomer units per chain was derived. This rather low value is supported by the solubility of the sample and the poor mechanical properties that we observed for this polymer while trying to make molds for dynamic mechanical measurements.

To check the occurrence of an increase in molecular weight taking place during an annealing at temperatures between T_g and T_f, the glass transition temperature was measured as a function of the annealing temperature. The results are shown in Figure 2 for a heat treatment of about 20–24 h in each case. The typical behavior of a polymer property with increasing molecular weight is observed. At annealing temperatures above about 453 K, the T_g first rises rapidly and then, at annealing temperatures close to T_f, reaches asymptotically its final value that is more than 10 deg above the glass transition temperature of the untreated polymer.

The final proof of a postcondensation with an attendant increase in molecular weight was obtained by performing viscosity measurements on the annealed samples. The results are also presented in Figure 2. As expected, the viscosity strongly increases with annealing temperature. In this figure the value for 553 K has to be considered with caution because the polymer annealed at this temperature was not completely soluble in the solvent mixture. Therefore, the insoluble part was extracted by filtration and the viscosity measured using the remaining solution. The "true" viscosity is thus expected to be even higher at this temperature.

It is known that the mechanical properties of LCP fibers, especially the tensile strength, improve significantly through annealing.[3] Such a heat treatment is an integral part of LCP fiber processing, as, for example, in the case of the HBA/HNA copolymer. Recently, it has been found that the molecular origin of this improvement is a postcondensation with an attendant increase in molecular weight[21] taking place under annealing. A fiber fracture originates mainly at the chain ends because of its inability to support the mechanical load concentration. Thus, decreasing the number of chain ends improves the mechanical performance of the fiber. This in return can be achieved by annealing the polymer since a decrease in the number of chain ends is directly related to an increase in the molecular weight. The fact that the present terpolyester undergoes a postcondensation by a simple secondary heating step is promising since it may well be accompanied by improvements in the mechanical properties. However, further experimental evidence is needed to support this idea.

X-ray Diffraction Experiments. Many of the stiff-chain thermotropic polymers that have been synthesized in the past exhibit sharp X-ray diffractions that can be associated with crystallites with three-dimensional order. As outlined in the foregoing section, such materials show two main transitions: a glass transition, T_g, usually at about 373–400 K and a melting point, T_f, usually greater than 500 K. The first of these transitions is accompanied by a change from a very rigid to a more flexible solid, while the second is associated with a change to a birefringent mesophase of very low viscosity. The solidlike behavior between T_g and T_f can be attributed to the crystallites which link the stiff chains together. In this sense, the crystals play the same role as they do in conventional semicrystalline polymers. A sufficiently long chain can thus connect various crystalline regions which, in the case of the copolymer of hydroxybenzoic acid and hydroxynaphthoic acid, are of the order of 5–10 nm in size. It has been shown, however, that when it comes to the detailed nature of the crystals, there are important distinctions such as the very low surface energy associated with the nematic chain morphology.[10] Since the molecular morphology, that is, the way chains pack and crystallize, is the underlying key to the behavior of LCP's and dictates to a large extent their macro- and micromorphological behavior, its knowledge is of great importance.

In recent years several X-ray diffraction investigations have been performed on the above terpolyester to elucidate its molecular morphology over the entire composition range. In a detailed study Erdemir *et al.*[22] have drawn attention to the various crystalline forms that can occur. Blundell *et al.*[11] have tried to relate the crystal structure to the nature of the phase diagram of the LCP. In the present paper the X-ray diffraction studies have two objectives. The first one is to estimate the overall crystallinity of the different samples, taking into account that each crystal form is associated with a particular sequence of comonomer units. It is well established that

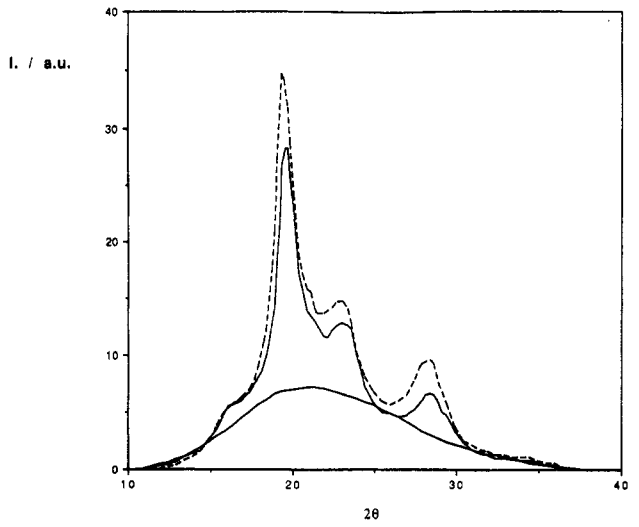

Figure 3. X-ray diffractograms of the HBA80 polymer: (—) untreated sample; (- - -) sample annealed during 7 days at 510 K. The diffractogram of the HBA33 sample is used to estimate the background diffraction from the noncrystalline regions.

motional parameters obtained from NMR experiments strongly depend on the solid-state organization.[23,24] This is a general property observed for a large number of semicrystalline polymers. It arises from differences in the strength of the dipolar interactions which are intense in the rigid crystalline parts and are motionally averaged at temperatures above T_g in the mobile amorphous parts of the sample. Thus to interpret the dynamical behavior observed for the different aromatic units in the NMR experiments, the information about the overall crystallinity is indispensable.

The second objective is to study the effects of prolonged annealing on the evolution of the different crystalline forms. As mentioned in the Introduction, it has been observed that on prolonged annealing, and depending on its composition, the terpolyester may undergo a crystalline reorganization.[17,18] In this paper a full account of these observations is given, leading to a better understanding of the nature of the crystal forms.

X-ray diffractograms taken from different samples in the terpolyester series reveal the existence of three distinct crystalline forms, in agreement with the observation of the authors cited above. In the following discussion we will adopt the notation I, II, and III for these forms as introduced by Blundell *et al.*, the main reflections from each form being listed in their paper.[11] Figure 3 shows two diffraction patterns of the HBA80 polymer, one recorded for a sample as obtained from the synthesis and the other for a sample annealed for 7 days at 510 K. To estimate the crystallinity, the diffractogram of the HBA33 polymer, precipitated from a 30/70 (v/v) mixture of trifluoroacetic acid and dichloromethane, is also depicted. After precipitation this polymer is amorphous, and, therefore, its diffractogram reflects the background diffraction from the noncrystalline regions. Measurements of the area above and below this line provide estimates of the crystallinity in each case; results thus obtained are listed in Table 1.

As can be seen on the diffractogram and indicated by the corresponding value in Table I, the HBA80 polymer is highly crystalline. The reflections observed for HBA80 (crystalline form III) are generally found for polymers with a high HBA content (>50% HBA) and are associated with oxybenzoate sequences. As can be deduced from Figure 3, long annealing times lead to higher crystallinity without appearance or disappearance of any reflection.

Table 1. Estimates for the Crystallinity of the Polymer Samples

polymer[a]	crystallinity (%)
HBA17 (1)	37
HBA17 (2)	38
HBA17 (3)	39
HBA27 (1)	19
HBA27 (2)	17
HBA27 (3)	18
HBA80 (1)	41
HBA80 (3)	48

[a] (1), untreated; (2), annealed for about 20 h at 510 K; (3), annealed for several days at 510 K (see text).

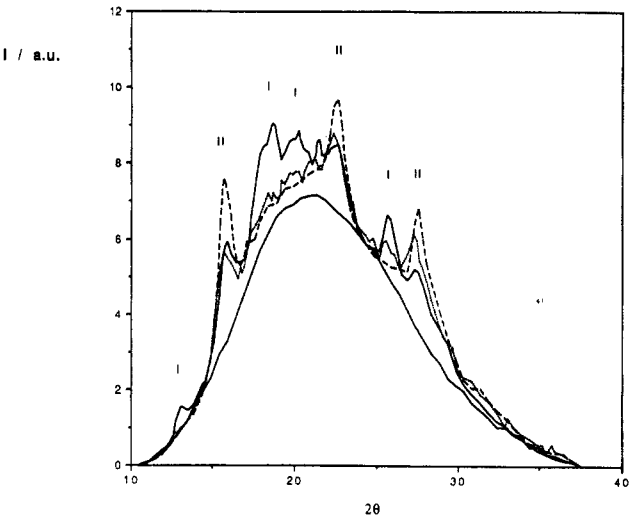

Figure 4. X-ray diffractograms of the HBA27 polymer: (—) untreated sample; (···) sample annealed for about 20 h at 510 K; (- - -) sample annealed for about 5 days at 510 K. The diffractogram of the HBA33 sample is used to estimate the background diffraction from the noncrystalline regions. The four main reflections of crystal form I and three main reflections of crystal form II are indicated in the figure.

Polymers having lower proportions of the HBA unit exhibit quite different X-ray patterns. Figure 4 shows the results obtained for the HBA27 sample. In addition to the diffractogram of the amorphous HBA33 polymer, three diffraction patterns of the HBA27 polyester are depicted. One is recorded for the polymer as obtained from the synthesis and the other two for samples annealed at 510 K for about 20 h and for 5 days, respectively. As expected, the crystallinity is much lower for HBA27 than for HBA80.

However, the most interesting observation is that the dominant crystalline form changes through annealing. Polymers having less than about 30% HBA units exhibit two distinct crystalline forms: I and II.[11] Both forms are associated with $(IA–HQ)_n$ sequences. Whereas the chain conformation of the sequence in form II is a fully extended zigzag with a cisoid type of arrangement of the ester groups around the isophthalic acid residue, the form I sequence likely takes on a less extended zigzag conformation. As can be seen from Figure 4, form I predominates in the as-made polymer although the main reflections of this form are not well developed since the overall crystallinity is rather low. After 20 h of annealing, one mainly observes a decrease in the intensities of the reflections of this crystalline form. Further annealing leads to a development of the reflections of form II. After 5 days at 510 K the only peaks left in the diffractogram are the three main reflections of this form. This behavior is also reflected by the estimated crystallinities reported in Table 1 that first slightly decrease and then slightly increase again on heating.

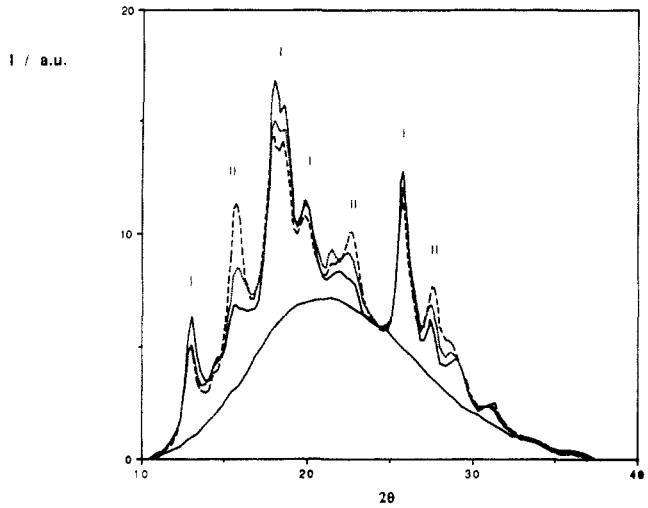

Figure 5. X-ray diffractograms of the HBA17 polymer: (—) untreated sample; (···) sample annealed for about 20 h at 510 K; (- - -) sample annealed for about 7 days at 510 K. The diffractogram of the HBA33 sample is used to estimate the background diffraction from the noncrystalline regions. The four main reflections of crystal form I and three main reflections of the crystal form II are indicated in the figure.

From their observations that form II is predominant in the middle composition range exhibiting a mesophase and that the original form I is converted into form II as a result of melt processing, Blundell *et al.*[11] deduced that form II is related to the liquid crystal mesophase. To check the validity of this assumption, we examined the HBA17 polymer annealed at 510 K for about 20 h and 7 days, respectively. This terpolyester is a conventional semicrystalline polymer showing no mesomorphic behavior. The result is depicted in Figure 5. Again the diffractograms of the two annealed samples are shown together with those of the unannealed sample and the amorphous HBA33 polyester. As can be seen from a comparison of the different figures and also from the values listed in Table 1, the crystallinity of HBA17 lies between that of the HBA80 and HBA27 polymers. In the diffractogram of the as-made polymer the four main reflections of crystalline form I as well as the three main reflections of form II can easily be recognized. The behavior after annealing is essentially the same as that observed for HBA27 although not as pronounced. Whereas the reflections of form I decrease, those of form II develop with longer annealing times. This experiment on the conventional semicrystalline HBA17 copolyester shows that the favoring of extended chain conformations through the nematic mesophase might support the development of crystals of form II but it is not the essential driving force of the reorganization.

Thermal Behavior. Before dealing with the NMR results, it is worthwhile to take a closer look at the thermal behavior of the investigated polymers. Figure 6 shows the DSC traces obtained from a first run of the untreated HBA27 and HBA80 samples. As can be seen, the thermogram of HBA80 is much more complex than that of HBA27, exhibiting several endothermic peaks at varying temperatures. Since NMR data will only be available up to about 510 K in the following, we will focus on the phenomena occurring below this temperature. Performing several runs up to 510 K on the HBA27 polymer leaves only one transition in the thermogram that looks like a glass transition. Therefore, the T_g is assigned to the 409 K transition. For HBA80 the assignment of T_g is more difficult. As shown in the previous section, HBA80 is highly crystalline, and, therefore, the manifestation of a

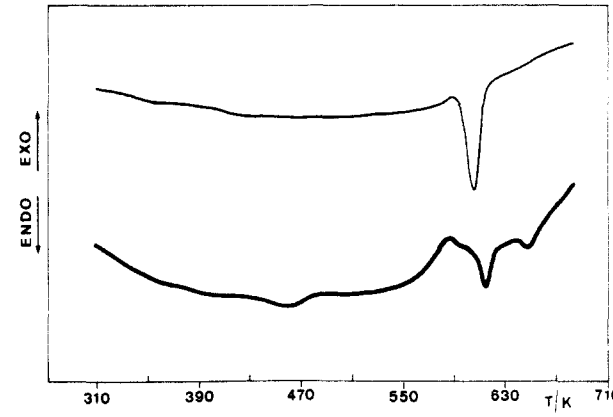

Figure 6. DSC thermograms as obtained from a first run of untreated HBA27 (upper trace) and untreated HBA80 (lower trace) samples.

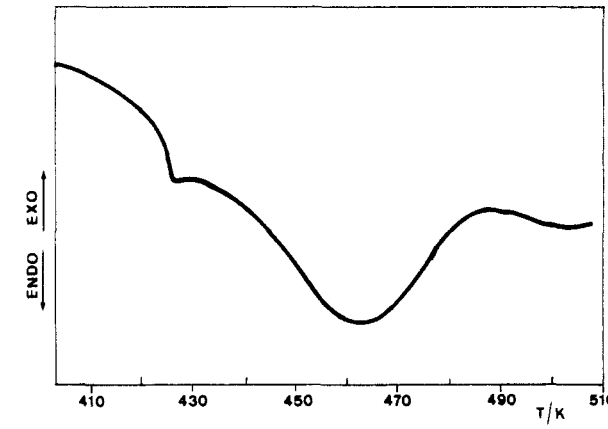

Figure 7. Enlargement of a DSC trace of the HBA80 polyester as obtained from a second run (first run: 273 → 523 K at a rate of 20 K/min).

glass transition in the DSC trace should be much weaker. Figure 7 shows an enlargement of a second DSC run of this polymer. A weak steplike behavior is observed at about 423 K in the DSC trace. It is followed by an endothermic peak centered at about 463 K. In the thermograms of the annealed samples used for the X-ray measurements, the first of these two effects was not detected.

To determine which of these phenomena is the glass transition, we have performed dynamic mechanical measurements on molds of the HBA80 polymer. The result is depicted in Figure 8. Since this polymer is very brittle and in addition the available amount of polymer was limited, only rather poor samples were obtained. This is why no absolute values of the tensile modulus E' are attached to the figure. However, a clear change in the temperature dependence of E' can be observed at about 423 K, indicating a softening of the material. This temperature coincides with the onset of the step behavior in the DSC trace of Figure 7. Therefore, the glass transition of the unannealed HBA80 sample can be assigned to the transition occurring at 423 K. The fact that this transition is not observed in the annealed samples may be due to the increasing crystallinity of the samples, thus preventing the detection of the T_g by DSC.

The glass transition temperatures of the different untreated polymers measured by DSC are listed in Table 2. It can be noticed that the T_g's of the strongly crystalline polymers are higher than those of the less crystalline ones. This can be explained by assuming that the crystalline regions of the highly crystalline polymers impose a

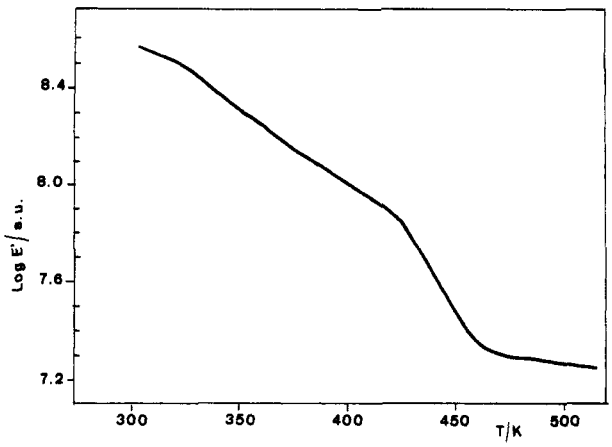

Figure 8. Tensile modulus E' as a function of temperature as obtained from dynamic mechanical measurements on molds of the HBA80 polymer.

Table 2. Glass Transition Temperature (T_g), of the Investigated Polymers

polymer	T_g(K)
HBA17	414
HBA27	409
HBA33	405
HBA80	425

constraint on the amorphous regions of the polymer. However, the molecular weights of the different polymers are not known, and in the section describing the post-condensation we have shown how strongly the T_g depends on this parameter. Therefore, one has to be careful in the interpretation of these data.

CP/MAS ^{13}C NMR Experiments. The remainder of this paper is devoted to the investigation of the local dynamics in the HBA80 and HBA27 polymers using high-resolution solid-state ^{13}C NMR spectroscopy. Taking into account the results obtained in the postcondensation study, the two polymers were annealed for about 20 h at 510 K prior to the NMR experiments; 510 K is about the highest temperature reached in the NMR investigation. The annealing ensures that the major part of the postcondensation reaction has already taken place prior to the measurements. Earlier kinetic studies on this terpolyester have shown that no transesterification can be detected at the temperatures used here.[17] Since, as mentioned above, a degradation of the polymers at temperatures up to 20 deg below the melting point is not observed, it can be concluded that no chemical reaction takes place during the NMR measurements.

Since the polymers have been annealed prior to the NMR experiments under the same conditions as those used for the X-ray investigation, the results discussed in this section can be used to estimate the crystallinity of the NMR samples. Taking NMR spectra at increasing temperatures is equivalent to an annealing of the polymers. This is especially true for higher temperatures where longer accumulation periods with the Doty probe head are necessary. Neglecting the influence of varying annealing temperatures, as a first approximation in the following we will assume that during the NMR investigation the polymers are in an intermediate state between the crystallinity displayed in the diffractograms taken after annealing for 20 h and several days, respectively, at 510 K.

Figure 9 shows representative high-resolution solid-state ^{13}C NMR spectra of HBA80 (Figure 9a) and HBA27 (Figure 9b). The line assignment is based on investigations described in ref 14. In the range between 115 and 170

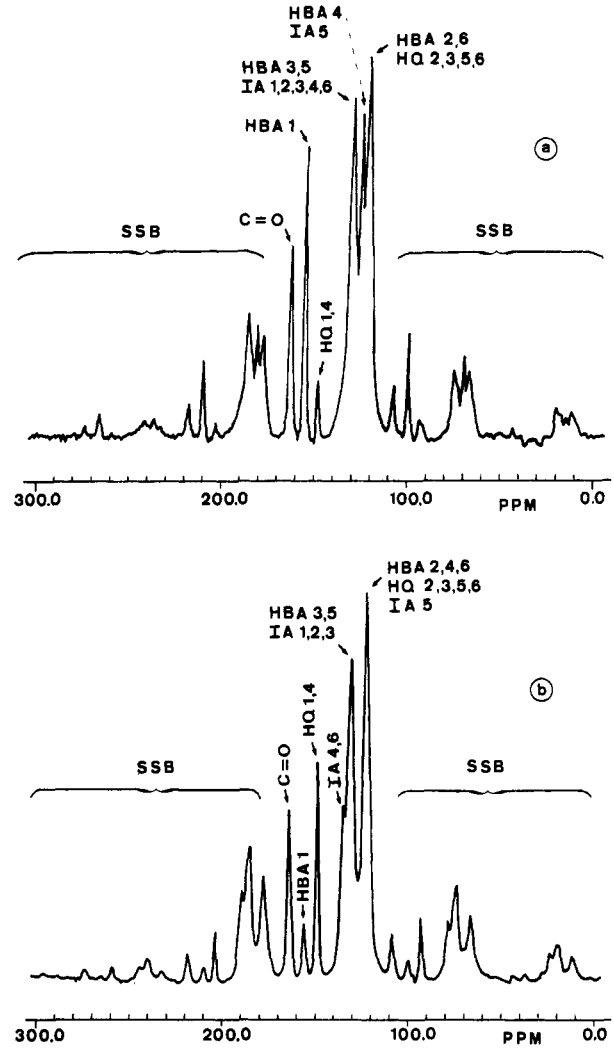

Figure 9. MAS/CP/DD ^{13}C NMR spectra of the HBA80 (a) and HBA27 (b) polymers at 363 K (SSB: spinning sidebands).

ppm, there are three well-separated lines. The peak at 148 ppm represents the resonances of carbons 1 and 4 of the HQ unit (HQ1,4), while the line at 154 ppm is characteristic of carbon 1 of the HBA unit (HBA1). Analysis of the spinning sidebands associated with these two peaks as a function of temperature provides information on the motional behavior of the phenylene rings of these two units. The peak at 164 ppm represents the resonances of all the carbonyl carbons of the terpolyester. A detailed analysis of the motional behavior of this polymer segment will be the subject of a subsequent publication. Since all resonances of the IA unit belong to either composite or very weakly resolved lines in the two spectra, information on the motion of the *meta*-substituted ring is not easily accessible.

Comparison of the two spectra drawn in Figure 9 shows that, as expected, the intensities of the two peaks at 154 and 148 ppm vary as a function of the copolyester composition. Consequently, the accuracy in the analysis of the motional behavior of the HBA80 polymer is larger for the HBA unit than for the HQ unit, whereas in the case of the HBA27 polymer the opposite is true.

CP/MAS ^{13}C NMR spectra were recorded under dipolar decoupling in the temperature range 213–510 K for the HBA80 polymer and 293–500 K for the HBA27 sample. The positions of the investigated peaks were independent of temperature. The relative intensities of the spinning sidebands decreased with increasing temperature, indicating the occurrence of local motions through a progressive

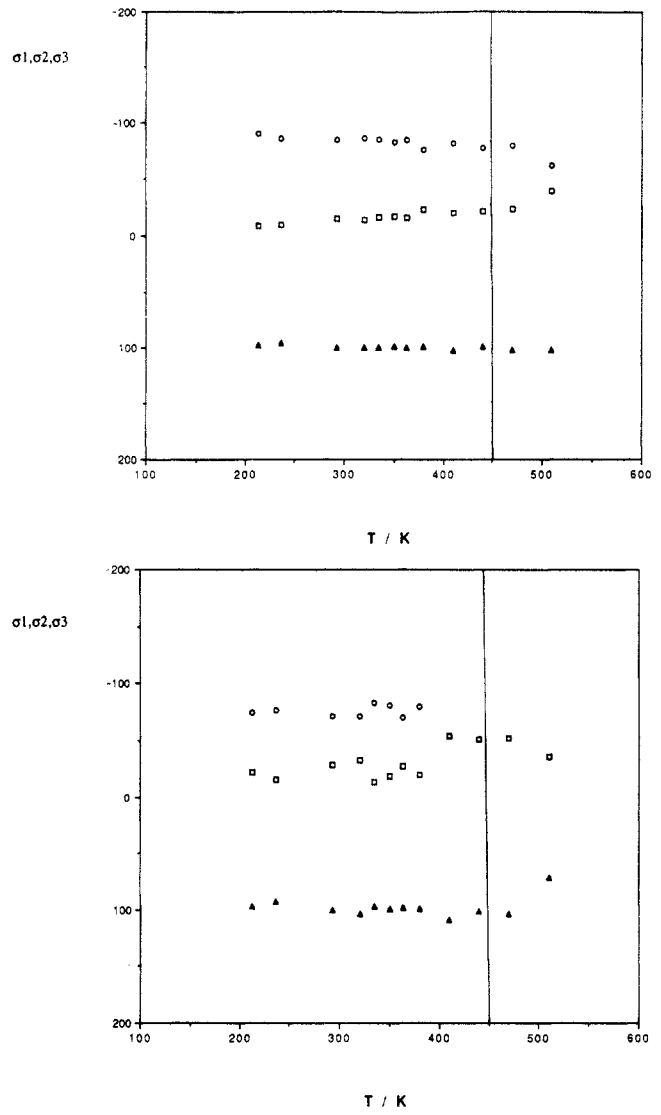

Figure 10. Principal elements σ_1 (△), σ_2 (□), and σ_3 (○) (expressed in ppm) of the chemical shift tensor of carbon 1 of the HBA unit (a top) and carbons 1 and 4 of the HQ unit (b, bottom) as a function of temperature for the HBA80 polymer. The extrapolated T_g of HBA80 is indicated as a vertical line.

averaging of the chemical shift tensor. In the following section, the temperature dependence of the principal elements of the chemical shift tensor will be determined using the method of Herzfeld and Berger.[16] The interpretation of the data in terms of molecular motions will be discussed.

(I) Local Dynamics of the HBA80 Polymer. The principal elements, σ_1, σ_2, and σ_3, of the chemical shift tensor of carbon 1 of the HBA unit and carbons 1 and 4 of the HQ unit, derived from the relative intensities of the spinning sidebands, are plotted as a function of temperature in Figure 10. As mentioned above and apparent from the two plots, as a result of the different intensities of the associated peaks, the scattering of the values is larger for the HQ unit than for the HBA unit. To check the results, especially those of the HQ unit, the high-temperature measurements were repeated twice starting from 373 K. The deviations from one series of measurements to the other lie within the experimental error that can be estimated from the fluctuations in the different plots.

The behavior of the two polymer units in the investigated temperature range is rather different. For carbon 1 of the HBA unit only a very weak temperature dependence can be observed. Whereas σ_1 remains constant, a slight decrease in σ_2 and a slight increase in σ_3 can be detected which is more pronounced between the two highest temperatures. On the other hand, a pronounced temperature dependence is found for the motional behavior of the HQ unit. For carbons 1 and 4 of this unit the values of σ_2 and σ_3 become equal for temperatures above 400 K. At the highest temperature the common value of σ_2 and σ_3 increases and σ_1 starts to decrease.

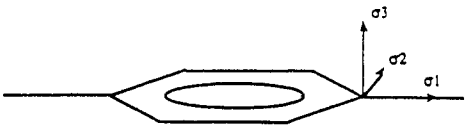

Figure 11. Orientation of the principal elements of the chemical shift tensor of an aromatic carbon (1 or 4) in a phenylene ring.

To interpret these results in terms of molecular motions, the orientation of the principal elements of the chemical shift tensor with respect to the molecular coordinate system has to be known. In the case of aromatic carbons the orientation has been determined from single-crystal studies.[25] The result is depicted in Figure 11. The least shielded element, σ_1, is in the aromatic plane pointing radially out from the ring, whereas the most shielded one, σ_3, is perpendicular to the ring plane. It has been shown that the orientations of the ^{13}C principal elements of aromatic carbons in different single crystals usually differ only by 1–2°.[26] In the following discussion we will therefore assume that the same orientation holds for the principal elements of the aromatic carbons investigated in this study. The results may then be interpreted in terms of an increasing mobility of the phenylene rings about the *para* axis leading to a progressive averaging of the σ_2 and σ_3 components. This type of rotational motion leaves σ_1 unchanged since it points in the direction of the local symmetry axis. The partial averaging of σ_2 and σ_3 for the HBA unit indicates either oscillations of restricted amplitude that increases with temperature or slow motions with a constant amplitude and an increasing rate which is not faster than the sensitivity of the NMR experiment in hertz. Equivalently, the complete averaging in the case of the HQ unit above 400 K indicates complete ring flips or very fast rates of motion.[14] The averaging of σ_1 and the common value of σ_2 and σ_3 for the HQ unit at the highest temperature correspond to an additional motion involving reorientations of the *para* axis of the ring.

At this point it is of interest to compare the NMR results with the thermal behavior of the HBA80 polymer described in the foregoing section. This requires the extrapolation of the low-frequency data to the higher frequencies of the NMR experiment.[24] The glass transition temperature of the untreated polymer measured at 1 Hz was found at 423 K. As viscoelastic data are not available for the HBA80 polyester, the coefficients of the William–Landel–Ferry equation[27] C_1^g and C_2^g have been estimated from dynamic mechanical measurements on other compositions of the terpolyester performed in our laboratory.[28] These experiments show that the terpolyesters lying in the middle composition range exhibit values of C_1^g and C_2^g comparable to those of amorphous polymers. The terpolyesters having low or high concentrations of HBA units exhibit higher values of C_1^g and C_2^g comparable to those of semicrystalline polymers. The extrapolation of the T_g was therefore performed assuming that the HBA80 coefficients are those of a semicrystalline polymer, that is, $C_1^g = 25$ and $C_2^g = 100$. The resulting T_g at the frequency of the NMR experiment, that is, 10^5 Hz, is indicated in Figure 10. As can be seen in this figure, the HQ unit shows the motional behavior that is expected to occur at the glass transition:

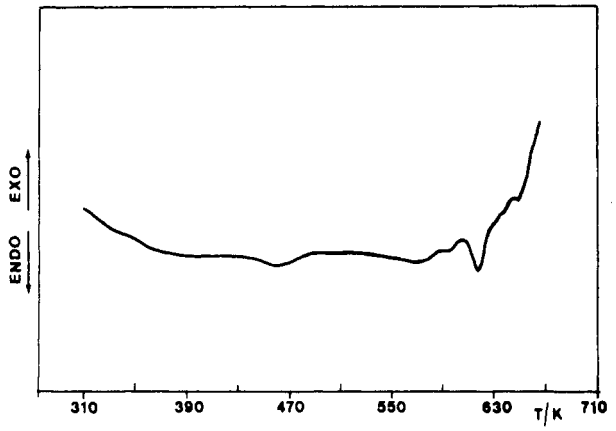

Figure 12. DSC thermogram of HBA80 annealed for about 20 h at 510 K as obtained from a first run.

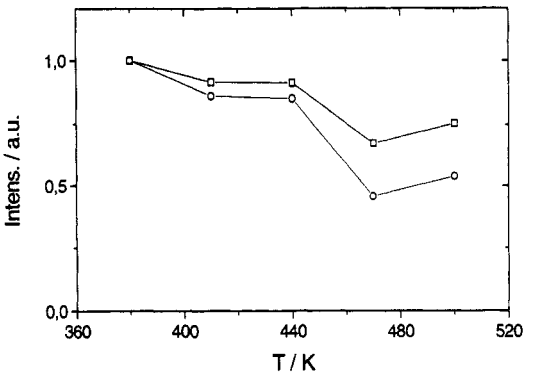

Figure 13. Normalized integrated intensity as a function of temperature for the peak at 154 ppm (□) representing the HBA units and for the peak at 148 ppm (○) representing the HQ segments.

the T_g lies in the temperature range above which an averaging of σ_1 and the common value of σ_2 and σ_3 of carbons 1 and 4 of this polymer segment set in. This result implies that the *para* axis of the phenyl ring starts to move in the frequency domain for which the NMR experiment is sensitive, indicating that the local mobility of the polymer main chain is activated at the T_g. Thus the glass transition found in the DSC measurement can be attributed to amorphous regions of the polymer that are rich in HQ.

For carbon 1 of the HBA unit an onset of chain mobility above the T_g involving a decrease of σ_1 is not detected. Instead, as indicated before, an acceleration in the decrease of σ_2 and the increase of σ_3 is observed. To explain this phenomenon, the thermogram of a HBA80 sample annealed for the NMR experiments is depicted in Figure 12. Compared to the thermogram of the untreated sample in Figure 6, a pronounced difference, especially in the multiple melting region around 590 K, can be detected. A closer look at this DSC trace reveals the beginning of a melting process at about 520 K. Considering that NMR is more sensitive to molecular motion than DSC, it is possible that the averaging phenomena observed for the HBA unit in Figure 10a at 510 K is due to a premelting process at this temperature.

In analogy to similar results obtained from NMR and dynamic mechanical measurements on the HBA33 terpolyester, the averaging of σ_2 and σ_3 of carbons 1 and 4 of the HQ unit around 400 K is assigned to a β secondary relaxation[14] involving a coupled motion of the *para*-substituted rings and carbonyl carbons. This relaxation is responsible for the drop in modulus observed in Figure 8 at temperatures below the glass transition temperature of HBA80.

From the NMR results one can conclude that the HBA unit is preferentially found in the crystalline regions of the polymer since its mobility is very restricted in the investigated temperature range whereas, as already discussed, the HQ unit is preferentially found in the amorphous regions showing greater mobility above the glass transition temperature. These observations correlate very well with the results of the X-ray diffraction experiments on the HBA80 polymer described above, since only those reflections were observed that are associated with sequences of the HBA unit. If the 50% crystallinity estimated from the X-ray investigation for samples annealed for several days is entirely due to crystals involving this unit, there are still almost 40% of this segment in noncrystalline regions of the HBA80 polymer. However, this value must be considered as an overestimation of the number of segments that contribute to the signal of the amorphous phase in the NMR experiments. Indeed, the percentage of rigid segments observed in NMR experiments is usually much larger than the degree of crystallinity since it may include very small crystallites that cannot be detected by X-ray diffraction as well as small regions in which the amorphous phase is constrained by its crystallite neighbors. The second reason why the contribution of these mobile segments above the T_g is not observed in Figure 10a is due to the cross-polarization sequence used to obtain the NMR spectra.[24] Once the temperature has passed T_g, the amorphous segments of the polymer start to move at increasing frequencies. In the intermediate motional regime the inverse of the correlation time of the motion approaches the intensity of the dipolar decoupling fields, in frequency units, and as a consequence the dipolar decoupling breaks down together with the cross-polarization efficiency. As an example, Rothwell has used the reduction of the efficiency of coherent averaging resulting from rf decoupling in the presence of incoherent averaging (molecular motion) for determining the rates and types of rotational motions in various materials.[29] In our case of a semicrystalline aromatic polymer where the resonances of one particular carbon resulting from amorphous and crystalline regions appear at the same chemical shift, these effects together lead to a discrimination against the more mobile parts of the sample, the main contribution to the detected signal above the T_g originating from the carbons in the rigid crystalline parts. Actually, as expected, a pronounced decrease in the signal to noise ratio passing T_g is detected not only for the peak at 148 ppm representing the HQ units preferentially found in the amorphous regions but also for the peak at 154 ppm representing the HBA segments as can be seen from Figure 13. To underline these arguments, it should be noted that in semicrystalline polyolefinic polymers, where signals originating from crystalline and amorphous parts can be distinguished via chemical shift, a pronounced decrease in signal intensity of the amorphous peaks can directly be observed at temperatures up to 100 K above T_g.[30]

(II) Local Dynamics of the HBA27 Polymer. For the HBA27 polymer σ_1, σ_2, and σ_3 of carbon 1 of the HBA unit and carbons 1 and 4 of the HQ unit as a function of temperature are plotted in Figure 14. Although not as apparent from the two plots as in the case of HBA80, it should be kept in mind that the accuracy in the analysis of the motional behavior of the HBA unit is much smaller than that of the HQ unit. As in the case of HBA80, the high-temperature measurements starting from 373 K were repeated twice. The observed fluctuations in the experi-

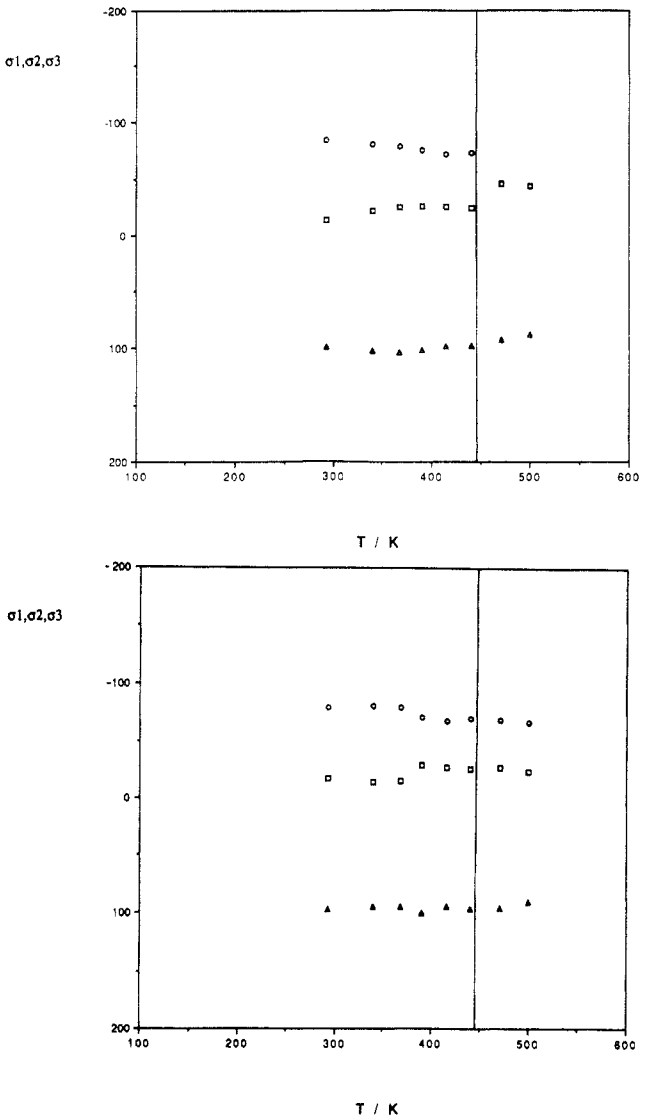

Figure 14. Principal elements σ_1 (Δ), σ_2 (□), and σ_3 (○) (expressed in ppm) of the chemical shift tensor of carbon 1 of the HBA unit (a, top) and carbons 1 and 4 of the HQ unit (b, bottom) as a function of temperature for the HBA27 polymer. The extrapolated T_g of HBA27 is indicated as a vertical line.

mental results were of the same order as in the case of HBA80. In contrast with results obtained for the HBA80 terpolyester, the HBA unit of the HBA27 polymer is more mobile than the HQ unit. As can be seen in Figure 14a, at temperatures up to about 450 K, for carbon 1 of the HBA unit σ_2 slowly decreases and σ_3 slowly increases whereas σ_1 stays unchanged. Above 450 K σ_2 and σ_3 become equal and their common value increases with increasing temperature whereas σ_1 decreases. For carbons 1 and 4 of the HQ unit the only significant evolution in the behavior of the principal elements of the chemical shift tensor can be observed somewhat below 400 K where σ_2 and σ_3 approach. Above this temperature, and until the highest temperature investigated, the three elements are nearly constant.

These observations may be interpreted in terms of the same local motions as those discussed for the HBA80 polymer, that is, a rotational motion about the local symmetry axis of the phenylene ring and a reorientation of this axis at temperatures above 450 K in the case of the HBA unit.

The glass transition temperature of the HBA27 polymer at the frequency of the NMR experiments is indicated on Figure 14. The estimation has been made using C_1^g and C_2^g coefficients comparable to those of amorphous polymers and found in our laboratory[28] for terpolyesters close in composition to the HBA27, that is, $C_1^g = 14$ and $C_2^g = 50$. In addition, the increase in the T_g as a result of the postcondensation studied in the first part of this work was taken into account. As in the case of the HQ unit of the HBA80 polymer, the T_g lies in the temperature range above which an averaging of σ_1 and the common value of σ_2 and σ_3 of carbon 1 of the HBA unit set in. For temperatures above the T_g the onset of motion of the *para* axis of the phenyl ring can be detected for this unit, indicating an increasing segmental mobility of the polymer chain. Thus, the glass transition observed on the DSC trace can be related to amorphous HBA-rich regions of the polymer.

As for the HBA unit in HBA80, passing the T_g does not have a significant effect on the values of the chemical shift tensor of carbons 1 and 4 of the HQ unit. Nevertheless, as in the former case, there occurs a pronounced decrease in the signal to noise ratio for the corresponding peaks of both units above the transition. The origin of the step observed in the motional behavior of the HQ unit somewhat below 400 K is not yet fully understood. It indicates an onset of mobility and seems to be a general phenomenon for the semicrystalline terpolyester. Further work is underway and the question will be resumed together with the analysis of the motional behavior of the carbonyl carbons in a subsequent publication.

From the results obtained in the NMR investigation of the HBA27 polymer it can be concluded that the more mobile HBA unit is preferentially found in the amorphous regions of this polymer whereas the more rigid HQ segment is preferentially found in the crystalline regions. This again correlates nicely with the results of the X-ray diffraction experiments on this polymer where only those crystal forms could be found that are associated with $(IA-HQ)_n$ sequences.

Conclusion

In the present study a number of different techniques have been used to characterize the thermal behavior, the molecular morphology, and the local dynamics of a series of semicrystalline terpolyesters incorporating kinked monomer units. The investigation of one polymer system varying only in the proportion of the different constituents has the advantage that it minimizes the number of parameters governing the behavior of the samples. This is of particular importance for the above polyester since its general behavior is rather complex. As an example, using X-ray diffraction we have shown that under annealing not only the overall crystallinity of these polymers increases but simultaneously, depending on the composition, a crystalline reorganization can be observed at longer times leading to a change in the dominant crystalline form. On a shorter time scale one has to take into account that a postcondensation with an attendant increase in molecular weight takes place which also changes the thermal behavior of the material. In the last part of the investigation we have shown that high-resolution solid-state ^{13}C NMR can be used to study the local dynamics of the HQ and HBA units of the semicrystalline terpolyesters. Correlations between the existence of different crystalline forms and the restriction of the local mobility of the associated polymer units were established. In addition, the increase in local mobility observed in the NMR measurements for units that were not associated with any crystalline forms could be related to the same type of motions found for the *para*-substituted phenylene rings in the amorphous ter-

polyester with $x = 0.33$, investigated in an earlier study.[14] These motions involve progressive ring oscillations around the *para* axis at lower temperatures and small-amplitude main-chain reorientations related to the glass transitions of the polymers evidenced by DSC and dynamic mechanical measurements. These results stress the interest of using a combination of different techniques to acquire a better understanding of the microscopic and macroscopic properties of these complex systems.

Acknowledgment. We thank F. Beaume, W. A. MacDonald, and N. Clough for the synthesis of the terpolymer samples and F. Queyroux and P. Tougne for assistance in performing the X-ray and NMR experiments, respectively. We are grateful to P. Sergot for the fabrication of the NMR rotors covering the whole temperature range of the experiments, especially for the low-temperature ones. We also thank C. Friedrich, C. Noël, and J. L. Halary for fruitful discussions.

References and Notes

(1) Ballauff, M. *Angew. Chem., Int. Ed. Engl.* **1989**, *28*, 253.
(2) See *Faraday Discuss. Chem. Soc.* **1985**, *79*.
(3) Yoon, H. N.; Charbonneau, L. F.; Calundann, G. W. *Adv. Mater.* **1992**, *4*, 206.
(4) Irvine, P. A.; Erman, B.; Flory, P. J. *J. Phys. Chem.* **1983**, *87*, 2929.
(5) Hummel, J. P.; Flory, P. J. *Macromolecules* **1980**, *13*, 479.
(6) Erman, B.; Flory, P. J.; Hummel, J. P. *Macromolecules* **1980**, *13*, 484.
(7) Hartmann, M.; Meyer, G.; Wöhrle, D. *Makromol. Chem.* **1975**, *176*, 831.
(8) Orthmann, E.; Enkelmann, V.; Wegner, G. *Makromol. Chem., Rapid Commun.* **1983**, *4*, 687.
(9) Schlüter, A. D. *Macromolecules* **1988**, *21*, 1208.
(10) Blundell, D. J. *Polymer* **1982**, *23*, 359.
(11) Blundell, D. J.; MacDonald, W. A.; Chivers, R. A. *High Perform. Polym.* **1989**, *1*, 97.
(12) Butzbach, G. D.; Wendorff, J. F.; Zimmermann, H. J. *Makromol. Chem., Rapid Commun.* **1985**, *6*, 821.
(13) MacDonald, W. A. *Mol. Cryst. Liq. Cryst.* **1987**, *153*, 311.
(14) Gérard, A.; Lauprêtre, F.; Monnerie, L. *Macromolecules* **1993**, *26*, 3313.
(15) Erdemir, A. B.; Johnson, D. J.; Karacan, I.; Tomka, J. G. *Polymer* **1988**, *29*, 597.
(16) Herzfeld, J.; Berger, A. E. *J. Chem. Phys.* **1980**, *73*, 6023.
(17) MacDonald, W. A.; McLenaghan, A. D. W.; Richards, R. W. *Macromolecules* **1992**, *25*, 826.
(18) McLean, G. Ph.D. Thesis, University of Durham, Durham, U.K., 1991.
(19) Stejskal, E. D.; Schaefer, J. *J. Magn. Reson.* **1975**, *18*, 560.
(20) Tegenfeldt, J.; Haeberlen, U.; Waugh, J. S. *J. Magn. Reson.* **1979**, *36*, 453.
(21) Yoon, H. N. *Colloid Polym. Sci.* **1990**, *268*, 230.
(22) Erdemir, A. B.; Johnson, D. J.; Tomka, J. G. *Polymer* **1986**, *27*, 441.
(23) Fyfe, C. A. *Solid State NMR for Chemists*; CFC Press: Guelph, ON, Canada, 1983.
(24) Lauprêtre, F. *Prog. Polym. Sci.* **1990**, *15*, 425.
(25) Pausak, S.; Pines, A.; Waugh, J. S. *J. Chem. Phys.* **1973**, *59*, 591.
(26) Veeman, W. S. *Prog. NMR Spectrosc.* **1984**, *16*, 193.
(27) Ferry, J. D. *Viscoelastic Properties of Polymers*; John Wiley: New York, 1980.
(28) Monnerie, L.; Halary, J. L., private communication.
(29) Rothwell, W. P.; Waugh, J. S. *J. Chem. Phys.* **1981**, *74*, 2721.
(30) Zemke, K. Ph.D. Thesis, University of Mainz, 1994.